Tetrahedron 68 (2012) 9694–9700

Contents lists available at SciVerse ScienceDirect

Tetrahedron

journal homepage: www.elsevier.com/locate/tet

Bioactive pregnane-type steroids from the soft coral *Scleronephthya gracillimum*

Hui-Yu Fang [a,†], Chih-Chuang Liaw [a,d,†], Chih-Hua Chao [a], Zhi-Hong Wen [a], Yang-Chang Wu [b], Chi-Hsin Hsu [a], Chang-Feng Dai [c], Jyh-Horng Sheu [a,d,*]

[a] *Department of Marine Biotechnology and Resources, National Sun Yat-sen University, Kaohsiung 804,Taiwan*
[b] *Graduate Institute of Integrated Medicine, China Medical University, Taichung 40402, Taiwan*
[c] *Institute of Oceanography, National Taiwan University, Taipei 106, Taiwan*
[d] *Asia Pacific Ocean Research Center, National Sun Yat-sen University, Kaohsiung 804, Taiwan*

ARTICLE INFO

Article history:
Received 4 June 2012
Received in revised form 11 September 2012
Accepted 11 September 2012
Available online 18 September 2012

Keywords:
Scleronephthya gracillimum
Sclerosteroids
O-Tolylthiocarbamate
Cytotoxic activity
Anti-inflammatory activity

ABSTRACT

Nine new steroids, sclerosteroids A–I (**1**, **5**, **6**, **8**–**13**), along with 18 known metabolites (**2**–**4**, **7**, **14**–**27**), were isolated from the soft coral *Scleronephthya gracillimum*. These structures were elucidated on the basis of detailed spectroscopic analysis. The absolute configurations of sugar moieties in steroidal glycosides **10**–**13** were determined by HPLC analysis of the *o*-tolylthiocarbamate derivatives of the liberated sugars from hydrolysis of these steroidal giycosides. Cytotoxic and anti-inflammatory activities of these compounds were measured in vitro.

1. Introduction

Soft coral of the genus *Scleronephthya* have been found to be an important source of pregnane-type steroids.[1–5] Some of the pregnanes possess important bioactivities, such as cytotoxic,[4–6] anti-inflammatory,[7] antiplasmodial,[8] and antibacterial activities.[9] In continuation of our previous studies of discovering bioactive steroids from soft corals,[10–19] the chemical investigation on *Scleronephthya gracillimum* was carried out and led to the isolation of 9 new pregnane-type steroids, sclerosteroids A–I (**1**, **5**, **6**, **8**–**13**), and 18 known compounds, stereonsteroid A (**2**),[4] ceratosteroid C (**3**),[20] ceratosteroid D (**4**),[20] pregna-1,20-dien-3-one (**7**),[21] 3-(4-*O*-acetyl-6-deoxy-β-galactopyranosyloxy)-19-norpregna-1,3,5(10),20-tetraene (**14**),[22] glaucasterol (**15**),[23] pregna-5,20-dien-3β-ol-3-acetate (**16**),[24] (5α,14α,17β)-pregn-20-en-3β-ol-3-acetate (**17**),[25] pregna-20-en-3-one (**18**),[21] 19-norpregna-1,3,5(10),20-tetraen-3-ol (**19**),[26] stereonsteroid H (**20**),[4] stereonsteroid G (**21**),[4] pregnene glycoside (**22**),[27] stereosteroid F (**23**),[4] pregn-20-en-3-*O*-α-fucopyranoside (**24**),[28] stereonsteroid E (**25**),[4] stereonsteroid D (**26**),[4] and ximasteroid D (**27**) (Fig. 1 and Supplementary data Fig. S1).[5] The structures of new compounds were established by extensive spectroscopic analysis and chemical methods. Among them, compound **1** showed significant cytotoxicity against human liver carcinoma (HepG2), human breast carcinoma (MDA-MB-231), meanwhile compounds **10**, **11**, **20**, and **26** were found to exhibit moderate cytotoxicity against human liver carcinoma (HepG2 and Hep3B), human breast carcinoma (MDA-MB-231 and MCF-7), human lung carcinoma (A-549), and human oral cancer (Ca9-22) cells. Besides, compounds **1**, **5**, **9**, **15**, and **23** could significantly inhibit the accumulation of the pro-inflammatory iNOS (inducible nitric oxide synthase) protein

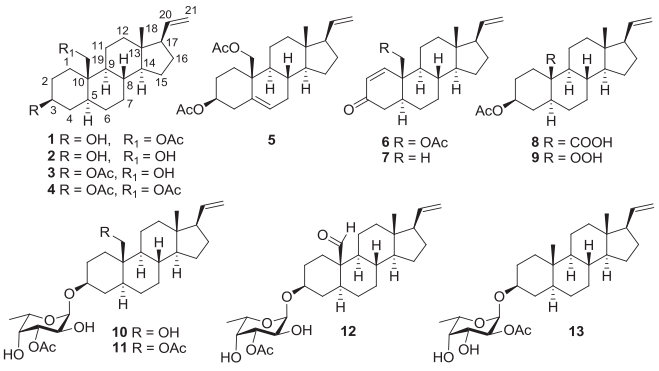

Fig. 1. Structure of new compounds isolated from *S. gracillimum*.

* Corresponding authors. Tel.: +886 7 5252000x5030; fax: +886 7 525 5020; e-mail address: sheu@mail.nsysu.edu.tw (J.-H. Sheu).
† These authors have the same contribution to the work.

0040-4020/$ – see front matter © 2012 Elsevier Ltd. All rights reserved.
http://dx.doi.org/10.1016/j.tet.2012.09.060

in LPS (lipopolysaccharide)-stimulated RAW264.7 macrophage cells. Compounds **1**, **5**, and **9** also showed activity in inhibiting the expression of COX-2 protein in the same cells.

2. Results and discussion

Sclerosteroid A (**1**) has a molecular formula of $C_{23}H_{36}O_3$ as determined by HRESIMS, appropriate for six degrees of unsaturation. The ^{13}C NMR and DEPT spectra of **1** showed the presence of 23 carbon signals, including 2 methyls, 10 sp^3 methylenes, 6 sp^3 methines, 1 sp^2 methine, 1 sp^2 methylene, and 1 sp^2 and 2 sp^3 quaternary carbons (Table 1). The ^1H NMR showed the presence of a tertiary methyl (δ_H 0.57, 3H, s), an acetoxymethyl (δ_H 4.21, 1H, d, J=12.0 Hz; 4.35, 1H, d, J=12.0 Hz; δ_H 2.06, 3H, s), a methine with an hydroxy group (δ_H 3.64, 1H, m), and a vinyl group (δ_H 4.95, 1H, br d, J=16.8 Hz; 4.96, 1H, br d, J=10.8 Hz; 5.74, 1H, ddd, J=16.8, 10.8, 7.6 Hz) (Table 1). These spectroscopic data showed that **1** might have a 3-hydroxy pregnane skeleton with an acetoxymethyl substituent at C-10 on the basis of the disappearance of a H_3-19 singlet around δ_H 0.80–1.10 and the presence of an AB doublet at δ_H 4.21 (J=12.0 Hz) and 4.35 (J=12.0 Hz). HMBC correlations from H_2-19 to C-10, C-9, C-5, and C-1 also confirmed this elucidation (Fig. S2). The relative stereochemistry of **1** was determined by the 2D NOE experiment (Fig. S3). The observed NOESY correlations between H-20 and H_3-18, H-14 and H-17, H_2-19 and H-8, H-9 and H-5 and H-3 revealed the β-orientation of H_3-18, H_2-19, and H-8 and the α-orientation of H-3, H-5, H-9, H-14, and H-17. On the basis of the above spectroscopic data, the structure of **1** was established as 19-acetoxy-5α-pregn-20-en-3-ol.

Compound **1** was identified to be the 19-acetylated derivative of **2** by comparison of their physical (optical rotation) and spectroscopic (^1H and ^{13}C NMR) data, meanwhile 3-acetylated **1** was also identical to **4** by comparison of their spectroscopic data. Due to the amount limitation, the absolute configuration of **1** was indirectly determined by the (*S*)- and (*R*)-α-methoxy-α-(trifluoromethyl) phenylacetic (MTPA) esters of **2** (**2a** and **2b**, respectively).[29,30] The values of $\Delta\delta$ [δ(*S*-MTPA ester of **2**)−δ(*R*-MTPA ester of **2**)] for H-3, H-4, and H-6 were positive, while the values of $\Delta\delta$ for H-1 and H-2 were negative, revealing the *S*-configuration at C-3 (Fig. 2).

Sclerosteroid B (**5**) has a molecular formula of $C_{25}H_{36}O_4$ as determined by HRESIMS, appropriate for six degrees of unsaturation.

Table 1
^1H and ^{13}C NMR spectroscopic data for compounds **1**, **5**, **6**, **8**, and **9**

No.	**1**			**5**			**6**			**8**			**9**		
	δ_C[a]	Mult.[c]	δ_H[d]	δ_C[a]	mult.[c]	δ_H[d]	δ_C[b]	Mult.[c]	δ_H[e]	δ_C[a]	mult.[c]	δ_H[d]	δ_C[a]	mult.[c]	δ_H[d]
1	31.9	CH_2	0.92 m 2.21 dt (13.6, 3.6)	31.5	CH_2	1.41 m 2.03 m	152.1	CH	7.01 d (10.5)	33.9	CH_2	1.05 m 2.51 dt (13.2, 3.2)	28.6	CH_2	1.12 m 2.61 dt (14.8, 3.2)
2	31.6	CH_2	1.30 m 1.85 m	25.4	CH_2	1.72 m 1.94 m	130.7	CH	6.04 d (10.5)	29.3	CH_2	1.53 m 1.94 m	27.4	CH_2	1.58 m 1.88 m
3	70.8	CH	3.64 m	70.0	CH	5.22 m	200.0	C		72.8	CH	4.76 ddd (16.0, 11.2, 4.8)	72.6	CH	4.74 m
4	38.4	CH_2	1.37 m 1.67 m	36.4	CH_2	1.55 m	41.5	CH_2	2.27 dd (18.0, 5.0) 2.58 dd (18.0, 14.5)	35.8	CH_2	1.50 m 1.82 m	34.0	CH_2	1.60 m 1.53 m
5	45.1	CH	1.29 m	145.0,	C		44.1	CH	2.03 m	44.3	CH	1.49 m	44.0	CH	1.48 m
6	28.2	CH_2	1.22 m 1.29 m	122.2	CH	5.47 br s	27.3	CH_2	1.56 m	28.5	CH_2	1.32 m	27.7	CH_2	1.28 m 1.47 m
7	32.0	CH_2	0.91 m 1.74 m	32.3	CH_2	2.09 m 2.20 m	31.4	CH_2	1.03 m 1.81 m	31.7	CH_2	0.94 m 1.79 m	31.8	CH_2	0.91 m 1.74 m
8	35.9	CH	1.48 m	33.1	CH	1.80 m	36.2	CH	1.56 m	35.9	CH	1.46 m	35.6	CH	1.71 m
9	54.6	CH	0.76 m	54.4	CH	0.88 m	50.3	CH	1.15 m	52.2	CH	0.93 m	52.4	CH	0.92 m
10	38.0	C		40.5	C		42.2	C		50.6	C		81.3	C	
11	21.8	CH_2	1.34 m 1.63 m	21.1	CH_2	1.34 m 1.60 m	21.3	CH_2	1.52 m 1.90 m	22.3	CH_2	1.35 m 1.74 m	22.4	CH_2	1.89 m 1.71 m
12	37.9	CH_2	0.97 m 1.67 m	37.6	CH_2	0.97 m 1.68 m	37.4	CH_2	1.08 m 1.79 m	37.4	CH_2	1.02 m 1.68 m	37.8	CH_2	0.95 m 1.69 m
13	43.6	C		43.5	C		43.6	C		43.5	C		43.5	C	
14	55.9	CH	0.99 m	55.6	CH	0.93 m	56.1	CH	1.03 m	55.7	CH	0.97 m	55.6	CH	1.01 m
15	24.7	CH_2	1.16 m 1.66 m	24.6	CH_2	1.18 m 1.67 m	24.6	CH_2	1.69 m	24.7	CH_2	1.23 m 1.73 m	24.9	CH_2	1.70 m 1.21 m
16	27.2	CH_2	1.54 m 1.77 m	27.1	CH_2	1.54 m 1.78 m	27.3	CH_2	1.56 m 1.78 m	27.2	CH_2	1.55 m 1.72 m	27.2	CH_2	1.58 m 1.79 m
17	55.3	CH	1.93 m	55.2	CH	1.91 m	55.2	CH	1.99 m	55.3	CH	1.96 m	55.3	CH	1.94 m
18	13.0	CH_3	0.57 s	12.9	CH_3	0.61 s	13.1	CH_3	0.63 s	13.0	CH_3	0.54 s	13.0	CH_3	0.66 s
19	62.9	CH_2	4.21 d (12.0) 4.35 d (12.0)	66.9	CH_2	4.14 d (11.2) 4.49 d (11.2)	62.1	CH_2	4.33 d (12.0) 4.48 d (12.0)	178.4	C				
20	139.8	CH	5.74 ddd (16.8, 10.8, 7.6)	139.6	CH	5.74 ddd (17.4, 10.4, 7.2)	139.4	CH	5.75 ddd (17.5, 10.5 7.5)	139.7	CH	5.73 ddd (16.8, 10.8, 7.6)	139.9	CH	5.76 ddd (16.4, 10.8, 7.6)
21	114.5	CH_2	4.95 br d (16.8) 4.96 br d (10.8)	114.7	CH_2	4.95 br d (17.4) 4.96 br d (10.4)	114.9	CH_2	4.97 br d (17.5) 4.98 br d (10.5)	114.6	CH_2	4.96 br d (16.8) 4.97 br d (10.8)	114.5	CH_2	4.96 br d (16.4) 4.97 br d (10.8)
OAc	171.2	C		171.0	C		170.7	C		170.7	C		170.8	C	
	21.2	CH_3	2.06 s	171.1	C		21.0	CH_3	1.95 s	21.4	CH_3	2.02 s	21.4	CH_3	2.03 s
				21.2	CH_3	2.05 s									
				21.4	CH_3	2.06 s									

[a] Recorded at 100 MHz in $CDCl_3$ at 25 °C.
[b] Recorded at 125 MHz in $CDCl_3$ at 25 °C.
[c] Multiplicities deduced by DEPT (The chemical shifts referenced to residual signal of $CDCl_3$ at δ 77.0 ppm.).
[d] Recorded at 400 MHz in $CDCl_3$ at 25 °C.
[e] Recorded at 500 MHz in $CDCl_3$ at 25 °C (The chemical shifts referenced to TMS at δ 0.0 ppm.).

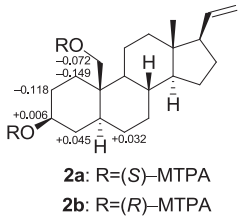

Fig. 2. ^{1}H NMR chemical shift differences $\Delta\delta$ ($\delta_S-\delta_R$) in parts per million for the MTPA esters of **2**.

The ^{13}C NMR and DEPT spectra of **5** showed the presence of twenty-five carbon signals, including three methyls, nine sp^3 methylenes, five sp^3 methines, two sp^2 methine, one sp^2 methylene, and three sp^2 and two sp^3 quaternary carbons (Table 1). The ^{1}H NMR spectra of **5** showed the presence of a tertiary methyl (δ_H 0.61, 3H, s), an acetoxymethyl (δ_H 4.14, 1H, d, J=11.2 Hz; 4.49, 1H, d, J=11.2 Hz; δ_H 2.06, 3H, s), a methine with an acetoxy group (δ_H 5.22, 1H, m; δ_H 2.05, 3H, s), a vinyl proton (δ_H 5.47, 1H, brs), and a terminal vinyl group (δ_H 4.95, 1H, br d, J=17.4 Hz; 4.96, 1H, br d, J=10.4 Hz; 5.74, 1H, ddd, J=17.4, 10.4, 7.2 Hz) (Table 1). These spectroscopic data showed that **5** might have a 3-*O*-acetoxyl-Δ5,6-pregnane skeleton with an acetoxymethyl substituent at C-10 on the basis of the disappearance of a H$_3$-19 singlet around δ_H 0.80–1.10 and the presence of an AB doublet at δ_H 4.14 (J=11.2 Hz) and 4.49 (J=11.2 Hz) and a broad-singlet vinyl proton (δ_H 5.47). The HMBC correlations from H$_2$-19 to C-10, C-9, C-5, and C-1 also confirmed this elucidation (Fig. S2). The relative stereochemistry of **5** was determined by the 2D NOE experiment. The observed NOESY correlations between H$_3$-18 and both H-20 and H-11β, H-14 and both H-17 and H-9, H$_2$-19 and H-8, and H-3 and H-1α revealed the β-orientation of H$_3$-18, H$_2$-19, and H-8 and the α-orientation of H-3, H-9, H-14, and H-17 (Fig. S3). On the basis of the above spectroscopic data, the structure of **5** was established as 3β,19-diacetoxypregna-5,20-diene.

Sclerosteroid C (**6**) was obtained as an amorphous solid. Its molecular formula, $C_{23}H_{32}O_3$, was established by HRESIMS, exhibiting eight degrees of unsaturation. The ^{1}H and ^{13}C NMR, involving the DEPT spectra, exhibited the presence of a tertiary methyl (δ_H 0.63 s; δ_C 13.1), a primary acetoxymethyl group (δ_H 4.33, 1H, d, J=12.0 Hz; 4.48, 1H, d, J=12.0 Hz; δ_C 62.1), a vinyl group (δ_H 4.97, 1H, br d, J=17.5 Hz; 4.98, 1H, br d, J=10.0 Hz; 5.75, 1H, ddd, J=17.5, 10.5, 7.5 Hz; δ_C 114.9, 139.4), and an α,β-unsaturated carbonyl group (δ_H 6.04, 1H, d, J=10.5 Hz; δ_H 7.01, 1H, d, J=10.5 Hz; δ_C 130.7, 152.1, and 200.0) (Table 1). From above data and extensive 2D NMR (Figs. S2 and S3) and CD data analysis,[31] **6** should be the 19-acetoxyl derivative of pregna-1,20-dien-3-one (**7**).[21]

HRESIMS of sclerosteroid D (**8**) exhibited a [M+Na]$^+$ peak at m/z 397.2355 (calcd for $C_{23}H_{34}O_4Na$, 397.2357) and established the molecular formula of $C_{23}H_{34}O_4$, implying seven degrees of unsaturation. The ^{1}H NMR spectroscopic data of **8** showed one characteristic methyl signal (δ_H 0.54, 3H, s), one oxymethine (δ_H 4.76, 1H, ddd, J=16.0, 11.2, 4.8 Hz), and a vinyl group (δ_H 4.96, 1H, br d, J=16.8 Hz; 4.97, 1H, br d, J=10.8 Hz; 5.73, 1H, ddd, J=16.8, 10.8, 7.6 Hz) (Table 1), revealing that **8** should have the same 3-acetoxy pregnane skeleton as **3**. Comparison of the ^{13}C NMR spectral data of **3** and **8** showed that the C-19 oxymethylene carbon (δ_C 60.8) in **3** was disappeared and replaced by a downfield-shifted carbonyl carbon (δ_C 178.4) in **8** and C-10 was downfield-shifted from δ_C 39.3 (in **3**) to 50.6 (in **8**), thus the C-19 carboxylic acid functionality of **8** was elucidated (Table 1). NOE correlations of **8** further established the relative stereochemistry of this steroid (Fig. S3), identical to those of **3** and **4**. From above data and extensive 2D NMR (Figs. S2 and S3), the structure of **8** was assigned as 3β-acetoxypregn-20-en-19-oic acid.

Sclerosteroid E (**9**) has a molecular formula of $C_{22}H_{34}O_4$ as determined by the HRESIMS and ^{13}C NMR spectroscopic data, deduced six degrees of unsaturation. The ^{1}H NMR spectroscopic data of **9** showed one methyl signal (δ_H 0.66, 3H, s), one oxymethine (δ_H 4.74, 1H, m), and a vinyl group (δ_H 4.96, 1H, br d, J=16.4 Hz; 4.97, 1H, br d, J=10.8 Hz; 5.76, 1H, ddd, J=16.4, 10.8, 7.6 Hz) (Table 1), revealing that **9** should have 3-acetoxy pregnane skeleton similar to that of **8**. Comparison of the ^{1}H and ^{13}C NMR spectral data of **8** and **9** showed that the C-19 carboxylic carbon (δ_C 178.4) in **8** was disappeared and C-10 was downfield-shifted from δ_C 50.6 (in **8**) to 81.3 (in **9**), while a proton signal was present at δ_H 6.97 (1H, br s) corresponding to a hydroperoxy group in **9**. The relative stereochemistry of **9** was further established by 2D NMR experiments, including HMBC and NOESY (Figs. S2 and S3). The NOE correlations of **9** between H$_3$-18 and H-8 suggested that H$_3$-18 and H-8 were β-oriented, also correlations between H-5 and H-9; H-17 and H-14 suggested that H-5, H-9, H-14, and H-17 were all α-oriented. The key NOE correlations of OOH-10 with H$_\beta$-4 and H-3 with H$_\alpha$-2 suggested both the hydroperoxy and acetoxy groups should be β-oriented. On the basis of the above analysis, the structure of **9** was established as 3β-acetoxy-19-nor-10β-hydroperoxypregn-20-ene.

The molecular formula of sclerosteroid F (**10**) was found to be $C_{29}H_{46}O_7$ by HRESIMS, DEPT, and ^{13}C NMR data, indicating seven degrees of unsaturation. The ^{1}H and ^{13}C NMR spectra of **10** displayed the signals for a vinyl group (δ_H 4.96, 1H, br d, J=17.2 Hz; 4.97, 1H, br d, J=10.0 Hz; 5.76, 1H, ddd, J=17.2, 10.0, 7.6 Hz; δ_C 114.5, 139.8), an ester carbonyl (δ_C 170.9), and an acetate methyl group (δ_H 2.17, 3H, s; δ_C 21.2). Therefore, **10** possesses five rings. The ^{1}H and ^{13}C NMR spectroscopic data of **10** were similar to those of **3** (Table 2), except for the appearing of six additional carbon signals at δ_C 97.3 (CH), 66.8 (CH), 73.9 (CH), 70.9 (CH), 65.8 (CH), and 16.0 (CH$_3$), an anomeric proton signal at δ_H 5.04 (1H, d, J=4.0 Hz), as well as a methyl doublet at δ_H 1.26, suggesting the presence of a 6′-deoxyhexose unit. This hexose appeared to be the C-3′ monoacetate derivative of fucopyranose by comparison of ^{1}H and ^{13}C NMR data with those reported previously[4] and on the basis of the results of ^{1}H–^{1}H COSY, HMBC, and NOESY experiments, in particular the HMBC correlation from H-3′ (δ_H 5.05) to the acetate carbonyl carbon (δ_C 170.9) (Fig. S2). The sugar was found to be connected to C-3 of the aglycon by HMBC correlation of H-1′ and C-3. The anomeric proton H-1′ (δ_H 5.04) has a small coupling constant, indicating the equatorial orientation of this proton. The relative configuration of the aglycon of **10** was further determined by NOESY experiment (Fig. S3). The absolute configuration of the sugar moiety in **10** was determined by reversed-phase HPLC analysis of its *o*-tolylisothiocarbamate.[32,33] The liberated fucose from acid hydrolysis of **10** was treated with L-cysteine methyl ester followed by reaction with *o*-tolylisothiocyanate to afford the corresponding *o*-tolylisothiocarbamate derivative. The retention time of this sugar derivative determined by HPLC analysis was found to be consistent with that of *o*-tolylisothiocarbamate derivative prepared from standard L-fucose. The structure of **10** was assigned as 3β-(3′-*O*-acetyl-α-L-fucopyranosyloxy)pregn-20-en-19-ol.

Sclerosteroid G (**11**) has a molecular formula, $C_{31}H_{48}O_8$, as determined by HRESIMS. The ^{1}H and ^{13}C NMR spectroscopic data of **11** resembled those of **10**, except that the presence of a primary hydroxy group at C-19 in **10** was replaced by a primary acetoxy group in **11** (Table 2). Acid hydrolysis of **11** also yielded L-fucose by HPLC analysis of its *o*-tolylisothiocarbamate derivative. The relative configuration and connection of the aglycon and sugar residue of **11** were further determined by ^{1}H–^{1}H COSY, HMBC, and NOESY experiments (Figs. S2 and S3). Thus, the structure of **11** was assigned as 3β-(3′-*O*-acetyl-α-L-fucopyranosyloxy)pregn-20-en-19-acetate.

Sclerosteroid H (**12**) had a molecular formula of $C_{29}H_{44}O_7$ as established by HRESIMS. The ^{1}H and ^{13}C NMR spectroscopic data of **12** were similar to those of **10**, except for the replacement of the

Table 2
^{1}H and ^{13}C NMR spectroscopic data for compounds **10**–**13**

No.	**10**			**11**			**12**			**13**		
	δ_C[a]	Mult.[b]	δ_H[c]	δ_C[a]	Mult.[b]	δ_H[c]	δ_C[a]	Mult.[b]	δ_H[c]	δ_C[a]	Mult.[b]	δ_H[c]
1	31.3	CH_2	0.83 m	32.0	CH_2	0.90 m	31.0	CH_2	0.96 m	37.5	CH_2	1.08 m
			2.28 dt (13.6, 3.6)			2.24 dt (13.6, 3.2)			2.42 dt (13.6, 3.6)			1.68 m
2	29.8	CH_2	1.50 m	29.4	CH_2	1.43 m	30.4	CH_2	1.39 m	29.3	CH_2	1.55 m
			1.90 m			1.86 m			1.94 m			1.79 m
3	77.4	CH	3.63 m	76.9	CH	3.62 m	76.9	CH	3.61 m	77.5	CH	3.50 m
4	34.9	CH_2	1.37 m	34.6	CH_2	1.32 m	36.0	CH_2	1.29 m	34.3	CH_2	1.27 m
			1.68 m			1.73 m			1.82 m			1.53 m
5	44.9	CH	1.20 m	44.9	CH	1.25 m	43.3	CH	1.39 m	44.8	CH	1.09 m
6	28.2	CH_2	1.21 m	28.2	CH_2	1.27 m	28.3	CH_2	1.52 m	28.8	CH_2	1.27 m
									1.92 m			
7	32.0	CH_2	0.90 m	31.9	CH_2	0.90 m	32.0	CH_2	1.06 m	32.2	CH_2	0.92 m
			1.70 m			1.73 m			1.89 m			1.72 m
8	36.1	CH	1.49 m	35.9	CH	1.48 m	37.0	CH	1.42 m	35.6	CH	1.39 m
9	54.9	CH	0.70 m	54.6	CH	0.73 m	52.8	CH	0.96 m	54.6	CH	0.68 m
10	39.4	C		38.1	C		51.8	C		35.7	C	
11	22.6	CH_2	1.51 m	21.8	CH_2	1.29 m	21.4	CH_2	1.26 m	20.8	CH_2	1.30 m
			1.67 m			1.61 m			1.73 m			1.54 m
12	38.0	CH_2	0.98 m	37.8	CH_2	0.92 m	37.3	CH_2	1.00 m	37.1	CH_2	1.01 m
			1.68 m			1.65 m			1.67 m			1.70 m
13	43.7	C		43.7	C		43.4	C		43.6	C	
14	55.8	CH	1.01 m	55.9	CH	0.98 m	55.7	CH	0.94 m	55.6	CH	0.99 m
15	24.7	CH_2	1.18 m	24.7	CH_2	1.18 m	24.6	CH_2	1.20 m	24.8	CH_2	1.17 m
			1.66 m			1.65 m			1.70 m			1.69 m
16	27.1	CH_2	1.54 m	27.1	CH_2	1.56 m	27.1	CH_2	1.55 m	27.2	CH_2	1.58 m
			1.77 m			1.78 m			1.78 m			1.80 m
17	55.4	CH	1.94 m	55.3	CH	1.92 m	55.3	CH	1.94 m	55.4	CH	1.94 m
18	13.3	CH_3	0.63 s	13.0	CH_3	0.58 s	12.8	CH_3	0.52 s	12.9	CH_3	0.61 s
19	60.8	CH_2	3.80 d (12.0)	62.7	CH_2	4.20 d (12.0)	208.4	CH	10.03 s	12.3	CH	0.84 s
			3.93 d (12.0)			4.37 d (12.0)						
20	139.8	CH	5.76 ddd (17.2,	139.8	CH	5.75 ddd (17.2,	139.5	CH	5.73 ddd (17.6,	139.9	CH	5.76 ddd (16.4,
			10.0, 7.6)			10.6, 8.0)			10.2, 7.6)			10.8, 8.0)
21	114.5	CH_2	4.96 br d (17.2)	114.5	CH_2	4.96 br d (17.2)	114.7	CH_2	4.97 br d (17.6)	114.3	CH_2	4.96 br d (16.4)
			4.97 br d (10.0)			4.97 br d (10.6)			4.98 br d (10.2)			4.98 br d (10.8)
1′	97.3	CH	5.04 d (4.0)	97.1	CH	5.03 d (4.0)	97.4	CH	5.00 d (3.6)	94.7	CH	5.13 d (3.6)
2′	66.8	CH	3.93 m	66.8	CH	3.90 dt (10.2, 4.0)	66.8	CH	3.90 m	72.1	CH	4.88 dd (10.2, 3.6)
3′	73.9	CH	5.05 dd (10.4, 2.8)	73.9	CH	5.04 dd (10.2, 2.8)	73.8	CH	5.02 dd (10.4, 3.6)	68.6	CH	4.02 dd (10.2, 3.2)
4′	70.9	CH	3.83 br s	70.9	CH	3.84 br s	71.0	CH	3.82 br s	72.4	CH	3.83 d (3.2)
5′	65.8	CH	4.10 q (6.6)	65.8	CH	4.09 q (6.8)	65.9	CH	4.06 q (6.4)	65.3	CH	4.13 q (6.4)
6′	16.0	CH_3	1.26 d (6.6)	16.0	CH_3	1.26 d (6.8)	16.0	CH_3	1.25 d (6.4)	16.1	CH_3	1.31 d (6.4)
OAc	170.9	C		170.7	C		170.8	C		171.5	C	
	21.2	CH_3	2.17 s	171.2	C		21.2	CH_3	2.16 s	21.1	CH_3	2.16 s
				21.2	CH_3	2.04 s						
				21.2	CH_3	2.18 s						

[a] Recorded at 100 MHz in $CDCl_3$ at 25 °C.
[b] Multiplicities deduced by DEPT (The chemical shifts referenced to residual signal of $CDCl_3$ at δ 77.0 ppm.).
[c] Recorded at 400 MHz in $CDCl_3$ at 25 °C (The chemical shifts referenced to TMS at δ 0.0 ppm.).

C-10 hydroxymethyl group in **10** by an aldehyde (δ_C 208.4; δ_H 10.03) in **12**, as also evidenced by the HMBC correlations from H-19 (δ_H 10.03) to C-10 (δ_C 51.8), C-9 (δ_C 52.8), C-5 (δ_C 43.3), and C-1 (δ_C 31.0) (Table 2). Acid hydrolysis of **12** also gave L-fucose as the sugar residue. The relative configuration and connection of the aglycon and sugar residue of **12** were further determined by $^{1}H-^{1}H$ COSY, HMBC, and NOESY experiments (Figs. S2 and S3). Thus, the structure of **12** was assigned as 3β-(3′-*O*-acetyl-α-L-fucopyranosyloxy) pregna-20-en-19-al.

Sclerosteroid I (**13**) has the molecular formula of $C_{29}H_{46}O_6$, determined by HRESIMS. The ^{1}H and ^{13}C NMR spectroscopic data of **13** resembled those of **12**, except for the presence of a methyl substituent at C-10 in **13** and the small variation in sugar moiety (Table 2). The sugar moiety of **13** was readily assigned to be the 2-*O*-acetyl-α-fucose by interpretation of $^{1}H-^{1}H$ COSY correlation together with an HMBC cross-peak from H-2′ to acetate carbonyl carbon (Fig. S2). The HMBC correlation from H-1′ (δ_H 5.13) to C-3 (δ_C 77.5) revealed that the sugar residue was attached to C-3 of the aglycon moiety (Fig. S2). Acid hydrolysis of **13** also liberated L-fucose. The relative configuration and connection of the aglycon and sugar residue of **13** were further determined by 2D NMR experiments (Figs. S2 and S3). Consequently, **13** was determined as 3β-(2′-*O*-acetyl-α-L-fucopyranosyloxy)pregna-20-ene.

The cytotoxicity of compounds **1**–**5**, **10**–**13**, **20**–**23**, **25**, and **26** against six human cancer cell lines, including hepatoma HepG2 and Hep3B cells, breast cancer MDA-MB-231 and MCF-7 cells, lung carcinoma A-549 cells, and gingival cancer Ca9-22 cells, was shown in Table 3. Among them, compound **1** exhibited stronger cytotoxicity against HepG2 and MDA-MB-23 with IC_{50} values of 19.5 and 15.8 μM, respectively. Compounds **10**, **11**, **20**, and **26** showed moderate cytotoxicity toward all six human cancer lines. Compounds **2**, **3**, **12**, **22**, and **23** showed selective moderate cytotoxicity toward hepatoma cells, HepG2 or Hep3B, and gingival cancer Ca9-22 cells, whereas these compounds showed inactive toward the other three cancer cell lines.

The anti-inflammatory activities of **1**–**5**, **7**–**27** were evaluated against the accumulation of pro-inflammatory iNOS and COX-2 proteins in RAW264.7 macrophage cells stimulated with LPS, which were measured by immunoblot analysis (Fig. 3). At a concentration of 10 μM, compounds **1**, **5**, and **9** significantly reduced the levels of iNOS protein to 28.4±9.4, 27.7±9.9%, and 25.4±6.4%, respectively, relative to control cells stimulated with LPS only,

Table 3
Cytotoxicity data of compounds isolated from *S. gracillimum*

Compound	Cell lines, IC_{50} (μM)					
	HepG2	Hep3B	Ca9-22	A-549	MCF-7	MDA-MB-231
1	19.5	[b]	[b]	26.7	[b]	15.8
2	45.7	44.4	39.3	—[a]	—[a]	—[a]
3	46.1	48.8	44.3	—[a]	—[a]	—[a]
4	36.8	35.3	34.7	46.2	42.2	—[a]
5	35.0	[b]	[b]	—[a]	[b]	41.3
10	35.6	29.3	28.9	30.6	38.7	30.8
11	29.0	28.1	27.2	28.7	34.1	28.0
12	—[a]	36.3	37.9	—[a]	—[a]	—[a]
13	37.4	31.5	30.8	28.9	—[a]	30.1
20	28.4	28.9	26.9	29.7	34.1	27.8
21	33.2	31.2	28.1	30.8	—[a]	32.0
22	32.1	30.3	28.4	—[a]	—[a]	—[a]
23	—[a]	32.2	37.3	—[a]	—[a]	—[a]
25	—[a]	—[a]	36.6	—[a]	—[a]	—[a]
26	23.5	26.8	24.7	28.9	31.0	27.0
Doxorubicin	0.3	1.1	0.3	1.9	2.2	2.1

[a] —, Inactive with IC_{50}>50 μM.
[b] Non-tested.

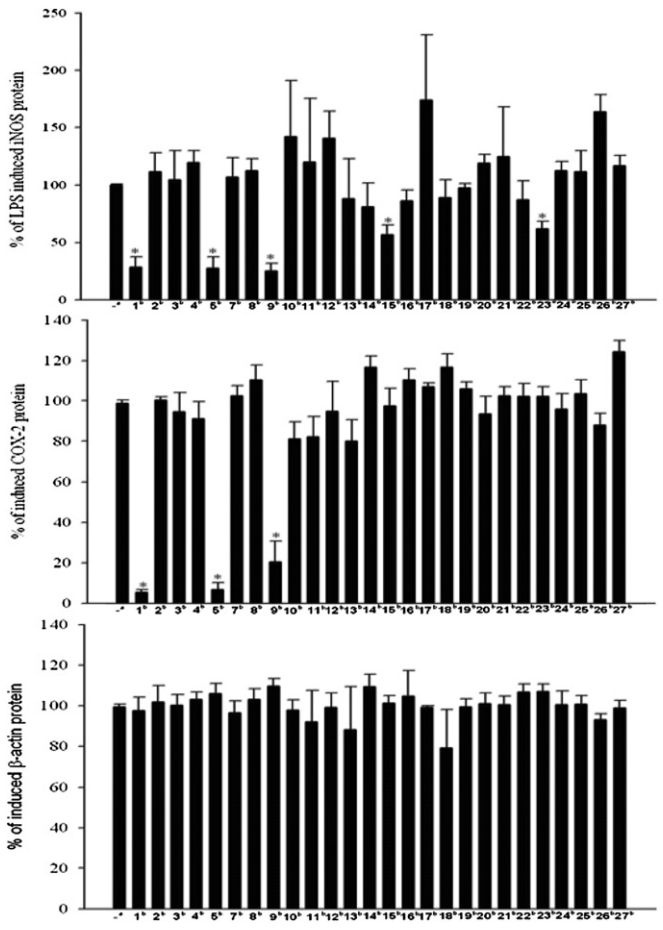

Fig. 3. Effect of isolates (10 μM) from *S. gracillimum* on the LPS-induced pro-inflammatory iNOS and on COX-2 protein expression of RAW264.7 macrophage cells by immunoblot analysis. (A) Quantification of immunoblots iNOS. (B) Quantification of immunoblots COX-2. The values are means±SEM (n=6). The relative intensity of the LPS alone stimulated group was taken as 100%. (C) Quantification of immunoblots of β-actin. *Significantly different from LPS alone stimulated group (*P<0.05). Control: stimulated with LPS.

meanwhile compounds **15** and **23** moderately reduced iNOS level to 56.7±4.4% and 61.9±6.5%, respectively. At this same concentration, compounds **1**, **5**, and **9** could reduce COX-2 expression to 5.4±1.3%, 6.7±3.5%, and 20.6±10.0%, respectively. Both results indicated that compounds **1**, **5**, and **9** might become the effective anti-inflammatory agents. None of the other compounds at 10 μM were inhibitory against the expression of pro-inflammatory iNOS and COX-2 proteins in RAW264.7 macrophage cells.

The present study demonstrates that the soft coral, *S. gracillimum*, can produce new pregnane-type metabolites, and some of these compounds showed useful anti-inflammatory effects. Thus, the chemical constituents of soft corals of this genus might be worthy of further investigation of discovering new bioactive agents.

3. Experimental

3.1. General experimental procedures

Melting points were determined using a Fisher-Johns melting point apparatus. Optical rotation was measured on a JASCO P1020 polarimeter. Ultraviolet spectra were recorded on a JASCO V-650 spectrophotometer. IR spectra were recorded on JASCO FT/IR-4100 infrared spectrophotometer. CD spectrum was measured on a JASCO J-815 spectrophotometer. The NMR spectra were recorded on a Bruker Avance 300 NMR spectrometer at 300 MHz for ^{1}H and 75 MHz for ^{13}C, on a Varian MR 400 NMR spectrometer at 400 MHz for ^{1}H and 100 MHz for ^{13}C, or on a Varian Unity INOVA 500 FT-NMR spectrometer at 500 MHz for ^{1}H and 125 MHz for ^{13}C. LRMS and HRMS were obtained by ESI on a Bruker APEX II mass spectrometer. Silica gel 60 (Merck, 230–400 mesh) was used for column chromatography. Precoated silica gel plates (Merck Kieselgel 60 F_{254} 0.2 mm) were used for analytical TLC. High-performance liquid chromatography was performed on a Hitachi L-7100 HPLC apparatus with a C-18 column (250×10 mm, 5 μm).

3.2. Material

The soft coral *S. gracillimum* was collected at Green Island, Taiwan, in January, 2008, at a depth of 10 m, and was stored in a freezer until extraction. A voucher specimen (NSYSU-SG001) was deposited in the Department of Marine Biotechnology and Resources, National Sun Yat-sen University.

3.3. Extraction and isolation

The frozen organisms (1.3 kg fresh wet) were sliced and extracted exhaustively with EtOH (3×2 L). The organic extract was concentrated to an aqueous suspension, which was further partitioned between EtOAc and water. The EtOAc extract (9.6 g) was fractionated by column chromatography on silica gel using *n*-hexane/EtOAc and EtOAc/MeOH mixtures of increasing polarity to yield 40 fractions. Fraction 5, eluting with *n*-hexane/EtOAc (60:1), was subjected to a Sephadex LH-20 column, using acetone as mobile phase, to afford two separated subfractions. Subfraction 1 was further separated by reversed-phase HPLC (MeOH/H_2O, 95:5) to afford **16** (2.5 mg) and **17** (4.1 mg). Fraction 12, eluting with *n*-hexane/EtOAc (6:1), was further separated by silica gel column chromatography (*n*-hexane/acetone, 10:1) and followed by reversed-phase HPLC (MeOH/H_2O, 85:15) to afford **4** (7.1 mg), **7** (1.4 mg), **18** (6.4 mg), and **19** (3.4 mg). Fraction 13, eluting with *n*-hexane/EtOAc (4:1), was further separated by silica gel column chromatography (*n*-hexane/EtOAc, 10:1) and followed by reversed-phase HPLC (MeOH/H_2O, 85:15) to afford **1** (8.0 mg), **5** (3.4 mg), **8** (2.7 mg), **9** (2.7 mg), and **15** (5.4 mg). Fraction 14, eluting with *n*-hexane/EtOAc (2:1), was further separated by silica gel column chromatography (*n*-hexane/EtOAc, 10:1) and followed by reversed-phase HPLC(MeOH/H_2O, 9:1) to afford **3** (13.4 mg) and **6** (0.7 mg). Fraction 18, eluting with *n*-hexane/EtOAc (1:6), was rechromatographed over a Sephadex LH-20 column using acetone as the mobile phase to afford six subfractions (A1–A6). Subfractions A2 and

A3 were combined and separated by reversed-phase HPLC (CH_3CN/H_2O, 9:1 to 3:1) to afford compounds **10** (6.2 mg), **11** (2.3 mg), **12** (8.1 mg), **13** (6.2 mg), **14** (1.7 mg), **2** (15.0 mg), **20** (13.4 mg), **21** (20.8 mg), **22** (8.7 mg), **23** (15.9 mg), **24** (1.5 mg), **25** (8.2 mg), **26** (14.3 mg), and **27** (3.7 mg).

*3.3.1. Sclerosteroid A (**1**).* Colorless gum; $[\alpha]_D^{25}$ −28.2 (*c* 0.4, $CHCl_3$); IR (KBr) ν_{max} 3403, 2927, 2866, 1738, 1448, 1240, and 1038 cm^{-1}; ^{13}C and ^1H NMR data, see Table 1 ESIMS *m*/*z* 383 $[M+Na]^+$; HRESIMS *m*/*z* 383.2562 $[M+Na]^+$ (calcd for $C_{23}H_{36}O_3Na$, 383.2560).

*3.3.2. Sclerosteroid B (**5**).* Colorless gum; $[\alpha]_D^{25}$ +72.4 (*c* 0.16, $CHCl_3$); IR (KBr) ν_{max} 2932, 2870, 1739, 1239, and 1025 cm^{-1}; ^{13}C and ^1H NMR data, see Table 1 ESIMS *m*/*z* 423 $[M+Na]^+$; HRESIMS *m*/*z* 423.2511 $[M+Na]^+$ (calcd for $C_{25}H_{36}O_4Na$, 423.2508).

*3.3.3. Sclerosteroid C (**6**).* Amorphous solid; $[\alpha]_D^{25}$ −29.2 (*c* 0.07, $CHCl_3$); IR (KBr) ν_{max} 2923, 2868, 1742, 1682, 1229, and 1036 cm^{-1}; UV (MeOH) λ_{max} (log ε) 226 (7.34) nm; CD (*c* 0.07, MeOH) λ_{max} ($\Delta\varepsilon$) 204 (−14.0), 230 (13.0), and 336 (−2.1); ^{13}C and ^1H NMR data, see Table 1 ESIMS *m*/*z* 379 $[M+Na]^+$; HRESIMS *m*/*z* 379.2249 $[M+Na]^+$ (calcd for $C_{23}H_{32}O_3Na$, 379.2250).

*3.3.4. Sclerosteroid D (**8**).* White powder; $[\alpha]_D^{25}$ −36.0 (*c* 0.10, $CHCl_3$); IR (KBr) ν_{max} 2945, 2868, 2842, 1733, 1687, 1242, and 1034 cm^{-1}; ^{13}C and ^1H NMR data, see Table 1 ESIMS *m*/*z* 397 $[M+Na]^+$; HRESIMS *m*/*z* 397.2355 $[M+Na]^+$ (calcd for $C_{29}H_{46}O_6Na$, 397.2357).

*3.3.5. Sclerosteroid E (**9**).* Colorless oil; $[\alpha]_D^{25}$ −13 (*c* 0.1, $CHCl_3$); IR (neat) ν_{max} 3390, 2926, 2864, 1718, 1447, 1250 and 1031 cm^{-1}; ^{13}C and ^1H NMR data, see Table 1 ESIMS *m*/*z* 385 $[M+Na]^+$; HRESIMS *m*/*z* 385.2355 $[M+Na]^+$ (calcd for $C_{22}H_{34}O_4Na$, 385.2357).

*3.3.6. Sclerosteroid F (**10**).* Amorphous solid; $[\alpha]_D^{25}$ −45.8 (*c* 0.11, $CHCl_3$); IR (KBr) ν_{max} 3452, 2925, 2868, 1723, 1377, 1249, 1072, and 1030 cm^{-1}; ^{13}C and ^1H NMR data, see Table 2 ESIMS *m*/*z* 529 $[M+Na]^+$; HRESIMS *m*/*z* 529.3141 $[M+Na]^+$ (calcd for $C_{29}H_{46}O_7Na$, 529.3144).

*3.3.7. Sclerosteroid G (**11**).* Amorphous solid; $[\alpha]_D^{25}$ −41.0 (*c* 0.16, $CHCl_3$); IR (KBr) ν_{max} 3453, 2935, 2868, 1736, 1372, 1240, 1073, and 1034 cm^{-1}; ^{13}C and ^1H NMR data, see Table 2 ESIMS *m*/*z* 571 $[M+Na]^+$; HRESIMS *m*/*z* 571.3247 $[M+Na]^+$ (calcd for $C_{31}H_{48}O_8Na$, 571.3245).

*3.3.8. Sclerosteroid H (**12**).* Amorphous solid; $[\alpha]_D^{25}$ −44.2 (*c* 0.12, $CHCl_3$); IR (KBr) ν_{max} 3440, 2936, 2869, 1720, 1380, 1245, 1073, 1035 cm^{-1}; ^{13}C and ^1H NMR data, see Table 2 ESIMS *m*/*z* 527 $[M+Na]^+$; HRESIMS *m*/*z* 527.2985 $[M+Na]^+$ (calcd for $C_{29}H_{44}O_7Na$, 527.2988).

*3.3.9. Sclerosteroid I (**13**).* Amorphous solid; $[\alpha]_D^{25}$ −14.2 (*c* 0.38, $CHCl_3$); IR (KBr) ν_{max} 3436, 2932, 2868, 1739, 1376, 1245, and 1046 cm^{-1}; ^{13}C and ^1H NMR data, see Table 2 ESIMS *m*/*z* 513 $[M+Na]^+$; HRESIMS *m*/*z* 513.3192 $[M+Na]^+$ (calcd for $C_{29}H_{46}O_6Na$, 513.3190).

*3.3.10. Pregna-1,20-dien-3-one (**7**).* $[\alpha]_D^{25}$ +31.5 (*c* 0.23, $CHCl_3$); lit. $[\alpha]_D$ +35.4 (*c* 0.5, $CHCl_3$);[21] CD (*c* 0.14, MeOH) λ_{max} ($\Delta\varepsilon$) 206 (−3.4), 238 (5.4), and 338 (−0.2); lit. CD (MeOH) $[\theta]_{237}$ 4770.[31]

*3.3.11. Acetylation of **1**.* A solution of **1** (1.9 mg) in pyridine (0.2 mL) was mixed with Ac_2O (0.1 mL), and the mixture was stirred at room temperature for 24 h. After evaporation of excess reagent, the residue was subjected to column chromatography over Si gel using *n*-hexane/EtOAc (4:1) to yield the diacetyl derivative **4** (2.5 mg, 91%), the specific rotation of which was in agreement with that of the natural product **4**.

*3.3.12. Acetylation of **2**.* To a stirring solution of **2** (5.0 mg) in pyridine (0.3 mL) was added Ac_2O (250 μL, 16 mg Ac_2O diluted in 2 mL pyridine). The mixture was quenched by H_2O (0.1 mL) after stirred over night at room temperature, and subsequently extracted by ethyl acetate. The organic layer was concentrated to give a residue, which was chromatographed on silica gel with *n*-hexane/EtOAc (8:1) as the eluent to afford 19-acetylated derivative (**1**, 0.7 mg), 3-acetylated one (**3**, 1.2 mg), 3,19-diacetylated one (**4**, 0.3 mg), and the recovered **2** (3.0 mg).

*3.3.13. Preparation of (S)-and (R)-MTPA esters of **2**.* To a solution of **2** (1 mg) in pyridine (0.4 mL) was added *R*-(−)-α-methoxy-α-(trifluoromethyl)phenylacetyl (MTPA) chloride (25 μL), and the mixture was allowed to stand over night at room temperature. The reaction was quenched by the addition of 1.0 mL of H_2O, and the mixture was subsequently extracted with EtOAc (3×1.0 mL). The EtOAc-soluble layers were combined, dried over anhydrous $MgSO_4$, and evaporated. The residue was subjected to short silica gel column chromatography over using *n*-hexane/EtOAc (3:1) to yield the (*S*)-MTPA ester, **2a** (0.8 mg, 87 %). The same procedure was used to prepare the (*R*)-MTPA ester, **2b** (0.7 mg, 76 %) from the reaction of (*S*)-MPTA chloride with **2** in pyridine. Selective ^1H NMR ($CDCl_3$, 400 MHz) of **2a**: δ 0.845 (1H, m, H-1a), 2.000 (1H, dt, *J*=13.6 and 3.6 Hz, H-1b), 1.753 (1H, m, H-2), 4.962 (1H, m, H-3), 1.418 (1H, m, H-4), 1.347 (1H, m, H-6), 1.154 (1H, m, H-6); Selective ^1H NMR ($CDCl_3$, 400 MHz) of **2b**: δ 0.917 (1H, m, H-1a), 2.149 (1H, dt, *J*=14.0 and 3.2 Hz, H-1b), 1.871 (1H, m, H-2), 4.956 (1H, m, H-3), 1.373 (1H, m, H-4), 1.290 (1H, m, H-6), 1.122 (1H, m, H-6).

3.3.14. Determination of sugar configuration. Authentic samples of D-fucose and L-cysteine methyl ester hydrochloride (each 0.5 mg) were dissolved in pyridine (0.1 mL) and heated at 60 °C for 1 h. To the mixture was added *o*-tolylisothiocyanate (0.5 mg in 0.1 mL pyridine) and heated at 60 °C for additional 1 h. The reaction mixture was directly analyzed by reversed-phase HPLC (Mightysil RP-18 GP column; 4.6×250 mm; 25% CH_3CN in 50 mM H_3PO_4; 0.5 mL/min; 35 °C) and detected at 250 nm to give the retention time of the *o*-tolylthiocarbamate of sugar. The retention time of the *o*-tolylthiocarbamate derived from L-fucose, L-cysteine methyl ester, and *o*-tolylisothiocyanate was obtained by the same manner.

A solution of the glycoside (0.3 mg for each) in 0.6 M HCl/dioxane (1:1 v/v, 0.2 mL) was heated at 90 °C for 4 h. After cooling, the solution was neutralized with Amberlite IRA400 (OH^- form), and the resin was removed by filtration. The filtrate was extracted with EtOAc. The aqueous layer was dried in vacuo and the afforded residue was dissolved in pyridine (0.1 mL) containing L-cysteine methyl ester (0.5 mg), followed by heating at 60 °C for 1 h. A 0.1 mL solution of *o*-tolylisothiocyanate (0.5 mg) in pyridine was added to the mixture, which was again heated at 60 °C for additional 1 h, to yield the corresponding *o*-tolylthiocarbamate derivative. Reversed-phase HPLC analysis of the *o*-tolylthiocarbamate derivatives derived from the hydrolyte of the glycosides **10**–**13** showed peaks at 42.3, 42.2, 42.3, and 42.8 min, respectively, while the t_R values for standard L-fucose and D-fucose derivatives were observed at 42.8 and 39.4 min, respectively, suggesting the presence of an L-fucose residue in **10**–**13**.

3.4. Cytotoxicity testing

Cell lines were purchased from the American Type Culture Collection (ATCC). Cytotoxicity assays were performed using the

MTT [3-(4,5-dimethylthiazole-2-yl)-2,5-diphenyltetrazolium bromide] colorimetric method.[34,35]

3.5. In vitro anti-inflammatory assay

Macrophage (RAW264.7) cell line was purchased from ATCC. In vitro anti-inflammatory activities of compounds **1**–**5**, and **7**–**27** were measured by examining the inhibition of LPS (lipopolysaccharide)-stimulated upregulation of iNOS (inducible nitric oxide synthase) and COX-2 (cyclooxygenase-2) proteins in macrophage cells using Western blot analysis.[36]

Acknowledgements

This work was supported by grants from the National Science Council of Taiwan NSC-100-2320-B-110-001-MY2 to J.-H.S.

Supplementary data

Structures of known compounds, ^{1}H and ^{13}C NMR spectra for **1**, **5**, **6**, **8**–**13** and their 2D NMR correlations. Supplementary data associated with this article can be found in the online version, at http://dx.doi.org/10.1016/j.tet.2012.09.060.

References and notes

1. Yan, X.-H.; Guo, Y.-W.; Zhu, X.-Z.; Mollo, E.; Cimino, G. *Youji Huaxue* **2004**, *24*, 1233–1238.
2. Kittakoop, P.; Suttisri, R.; Chaichantipyuth, C.; Vethchagarun, S.; Suwanborirux, K. *J. Nat. Prod.* **1999**, *62*, 318–320.
3. Han, L.; Wang, C.-Y.; Huang, H.; Shao, C.-L.; Liu, Q.-A.; Qi, J.; Sun, X.-P.; Zhai, P.; Gu, Y.-C. *Biochem. Syst. Ecol.* **2010**, *38*, 243–246.
4. Wang, S.-K.; Dai, C.-F.; Duh, C.-Y. *J. Nat. Prod.* **2006**, *69*, 103–106.
5. Yan, X.-H.; Liu, H.-L.; Guo, Y.-W. *Steroids* **2009**, *74*, 1061–1065.
6. Ioannou, E.; Abdel-Razik, A. F.; Alexi, X.; Vagias, C.; Alexis, M. N.; Roussis, V. *Tetrahedron* **2008**, *64*, 11797–11801.
7. Chao, C.-H.; Wen, Z.-H.; Su, J.-H.; Chen, I. M.; Huang, H.-C.; Dai, C.-F.; Sheu, J.-H. *Steroids* **2008**, *73*, 1353–1358.
8. Gutiérrez, M.; Capson, T. L.; Guzmán, H. M.; González, J.; Ortega-Barría, E.; Quiñoá, E.; Riguera, R. *J. Nat. Prod.* **2006**, *69*, 1379–1383.
9. Diaz-Marrero, A. R.; Porras, G.; Aragón, Z.; de la Rosa, J. M.; Dorta, E.; Cueto, M.; D'Croz, L.; Maté, J.; Darias, J. *J. Nat. Prod.* **2011**, *74*, 292–295.
10. Lu, Y.; Lin, Y.-C.; Wen, Z.-H.; Su, J.-H.; Sung, P.-J.; Hsu, C.-H.; Kuo, Y.-H.; Chiang, M. Y.; Dai, C.-F.; Sheu, J.-H. *Tetrahedron* **2010**, *66*, 7129–7135.
11. Chao, C.-H.; Wen, Z.-H.; Chen, I. M.; Su, J.-H.; Huang, H.-C.; Chiang, M. Y.; Sheu, J.-H. *Tetrahedron* **2008**, *64*, 3554–3560.
12. Su, J.-H.; Lo, C.-L.; Lu, Y.; Wen, Z.-H.; Huang, C.-Y.; Dai, C.-F.; Sheu, J.-H. *Bull. Chem. Soc. Jpn.* **2008**, *81*, 1616–1620.
13. Chen, B.-W.; Su, J.-H.; Dai, C.-F.; Wu, Y.-C.; Sheu, J.-H. *Bull. Chem. Soc. Jpn.* **2008**, *81*, 1304–1307.
14. Su, J.-H.; Lin, F.-Y.; Dai, C.-F.; Wu, Y.-C.; Hsu, C.-H.; Sheu, J.-H. *Bull. Chem. Soc. Jpn.* **2007**, *80*, 2208–2212.
15. Su, J.-H.; Lin, F.-Y.; Huang, H.-C.; Dai, C.-F.; Wu, Y.-C.; Hu, W.-P.; Hsu, C.-H.; Sheu, J.-H. *Tetrahedron* **2007**, *63*, 703–707.
16. Ahmed, A. F.; Hsieh, Y.-T.; Wen, Z.-H.; Wu, Y.-C.; Sheu, J.-H. *J. Nat. Prod.* **2006**, *69*, 1275–1279.
17. Su, J.-H.; Tseng, Y.-J.; Huang, H.-H.; Ahmed, A. F.; Lu, C.-K.; Wu, Y.-C.; Sheu, J.-H. *J. Nat. Prod.* **2006**, *69*, 850–852.
18. Chao, C.-H.; Huang, L.-F.; Yang, Y.-L.; Su, J.-H.; Wang, G.-H.; Chiang, M. Y.; Wu, Y.-C.; Dai, C.-F.; Sheu, J.-H. *J. Nat. Prod.* **2005**, *68*, 880–885.
19. Sheu, J.-H.; Chao, C.-H.; Wang, G.-H.; Hung, K.-C.; Duh, C.-Y.; Chiang, M. Y.; Wu, Y.-C.; Wu, C.-C. *Tetrahedron Lett.* **2004**, *45*, 6413–6416.
20. Lu, C.-K.; Wang, S.-K.; Duh, C.-Y. *Bull. Chem. Soc. Jpn.* **2011**, *84*, 943–946.
21. Seo, Y.; Jung, J. H.; Rho, J.-R.; Shin, J.; Song, J.-I. *Tetrahedron* **1995**, *51*, 2497–2506.
22. Tomono, Y.; Hirota, H.; Imahara, Y.; Fusetani, N. *J. Nat. Prod.* **1999**, *62*, 1538–1541.
23. Kobayashi, M.; Shizaka, T.; Mitsuhashi, H. *Chem. Pharm. Bull.* **1983**, *31*, 1803–1805.
24. Kingston, J. F.; Gregory, B.; Fallis, A. G. *J. Chem. Soc., Perkin Trans. 1* **1979**, 2064–2068.
25. Higg, M. D.; Faulkner, D. J. *Steroids* **1977**, *30*, 379–388.
26. Blackman, A. J. H. A.; Skelton, B. W.; White, A. H. *Aust. J. Chem.* **1985**, *38*, 565–573.
27. Cóbar, O. M.; Rodríguez, A. D.; Padilla, O. L. *J. Nat. Prod.* **1997**, *60*, 1186–1188.
28. Huang, X. P.; Deng, Z. W.; Ofwegen, L. V.; Li, J.; Fu, H. Z.; Zhu, X. B.; Lin, W. H. *J. Asian Nat. Prod. Res.* **2006**, *8*, 287–291.
29. Ohtani, I.; Kusumi, T.; Kashman, Y.; Kakisawa, H. *J. Am. Chem. Soc.* **1991**, *113*, 4092–4096.
30. Ohtani, I.; Kusumi, T.; Kashman, Y.; Kakisawa, H. *J. Org. Chem.* **1991**, *56*, 1296–1298.
31. Schow, S. R.; McMorris, T. C. *Steroids* **1977**, *30*, 389–392.
32. Tanaka, T.; Nakashima, T.; Ueda, T.; Tomii, K.; Kouno, I. *Chem. Pharm. Bull.* **2007**, *55*, 899–901.
33. Chao, C.-H.; Chou, K.-J.; Huang, C.-Y.; Wen, Z.-H.; Hsu, C.-H.; Wu, Y.-C.; Dai, C.-F.; Sheu, J.-H. *Mar. Drugs* **2012**, *10*, 439–450.
34. Alley, M. C.; Scudiero, D. A.; Monks, A.; Hursey, M. L.; Czerwinski, M. J.; Fine, D. L.; Abbott, B. J.; Mayo, J. G.; Shoemaker, R. H.; Boyd, M. R. *Cancer Res.* **1988**, *48*, 589–601.
35. Scudiero, D. A.; Shoemaker, R. H.; Paull, K. D.; Monks, A.; Tierney, S.; Nofziger, T. H.; Currens, M. J.; Seniff, D.; Boyd, M. R. *Cancer Res.* **1988**, *48*, 4827–4833.
36. Chao, C.-H.; Wen, Z.-H.; Wu, Y.-C.; Yeh, H.-C.; Sheu, J.-H. *J. Nat. Prod.* **2008**, *71*, 1819–1824.